Optimization of CMT Cladding Process Parameter Using COPRAS Method in Cladding of Stellite-6 on AISI316L Alloy

Thinesh Babu Thiagarajan[1], Sengottuvel Ponnusamy[2]

[1]Research Scholar& Mechanical Engineering & Bharath Institute of Higher Education and Research, Chennai 600073 India
[2]Research Supervisor& Mechanical Engineering & Bharath Institute of Higher Education and Research, Chennai 600073 India

[1]thineshbabu@outlook.com

Abstract - This paper discusses the optimization of the welding parameter of the cold arc metal transfer (CMT) cladding process using a new technique called complex proportional assessment (COPRAS). The experiments were done based on central composite design (CCD). Welding speed, torch angle, current, and volt were the welding parameters for the experiment. The corrosion rate analysis, microhardness, microstructure, and the EDS x-ray spectroscopy analysis of the optimized parameters are discussed here based on COPRAS optimization ranking. Here, the cobalt-based alloy stellite-6 was coated over the AISI316L alloy. The results showed that the optimized experiment yielded good microhardness on cladding, interface and SS316L base metal sides and a maximum hardness of 350Hv observed in the cladding surface. From the EDS analysis of the cladding of experiment 23, the Cr and Co phases were found. The weld interface value varies from 0.04 to 0.19 mm.

Keywords - *AISI316L, Cladding, CMT, COPRAS Optimization, Stellite-6*

I. INTRODUCTION

The COPRAS method was developed by Zavadskas et al. [1, 2]that involves proportional & direct dependence on the significance, the worthiness of available alternatives in the existence of mutually distinct parameters. COPRAS considers the triumph of available alternatives through various parameters also the associated influences with the help of a systematic ranking/grade and formative system. The variant choice that ranked in the COPRAS method considers their relevance and their degree of usefulness to the present problem. Variety of engineering applications that propose dynamic decision-making problems can be dealt with with COPRAS methodology [3]. Machine tool selection is also possible in the best way by the COPRAS method. Compared to other MCDM techniques, COPRAS is advantageous since it is easy to use and friendliness. This method also possesses some drawbacks while dealing with qualitative data and characteristics [4]. Audrius Cereska et al. [5] studied metal screw manufacturing by different materials using several decision-making techniques like "Technique for Order of Preference by Similarity to Ideal Solution" (shortly called "TOPSIS"), COPRAS, additive weighting (AW). Jagannath Roy et al. [6] solved Multi-Criteria Decision Making (called "MCDM") problems using the COPRAS method to evaluate the tourist hotels under the list of preferences needed and select the best hotels as per the ranking the application of COPRAS is also identified in the welding research. S.Nweze and J.Achebo [7] used the COPRAS for their research on the improvement of the performance of mild steel weldment using tungsten inert gas welding. They optimized the welding process parameters by the hybrid method COPRAS cum addition ratio assessment method (ARAS). Through this method, they found the optimized weld parameters. M.Gomathisankar et al. [8] Researched the optimization of aluminum alloy welding parameters using the COPRAS- MCDM method to determine the best combinations for the properties. The authors used the analysis of variance (ANOVA) with COPRAS for identifying the contribution percentage. The COPRAS can be used in the additive manufacturing technique also. Makhesana M.A. [9] successfully applied the COPRAS method for selecting the prototyping parameters. The application of austenitic stainless steel like 304 and 316 have versatile applications in marine, automobile, and aerospace research as those having weldability and excellent corrosion properties [10]. The combination of Stellite and stainless steel for the cladding process is recommended [11]. Many welding techniques like laser, MIG, and TIG are used for the cladding of one metal over another one [12]. CMT process is one of the advanced metal inert gas welding (MIG) [13] and is suitable in industries for improving the cladding performance. F.Madadi et al. [14] optimized the stellite cladding by TIG using the Response-Surface-Methodology(called "RSM"). The authors created a model for the optimization and analyzed the significance using ANOVA. The combination of ANOVA with other optimization methods is popular in choosing the welding parameters. Dariusz Bartkowski et al. [15] investigated the laser cladding performance of stellite-6 alloy and found that the coating achieved maximum hardness, and the bonding was good. Anish Nair et al. [16] proposed new fuzzy modeling for the stellite

cladding on steel using a laser process. Through this fuzzy model, the authors optimized the corrosion resistance index with the help of the Taguchi method. A vast literature that discussed the laser cladding process was found through the literature survey as laser improves the performance. But the method of CMT cladding is limited.

In this work, the cladding of stellite-6 was clade 31 times differently over the SS316L alloy of using the CMT process according to the welding parameters framed by CCD. Further, the parameters were optimized using the method COPRAS for identifying the best experiment by the ranking system. Based on the ranks, the first, middle, and rank specimens were characterized for the macro and microstructure, EDS, Vickers hardness, and corrosion rate analysis. The results are explained in this paper. The usage of COPRAS in welding and cladding area is still limited. The main aim of this paper is to express the application of COPRAS optimization and its ranking results in welding and surface applications.

II. MATERIALS AND METHOD

Stellite-6 is a cobalt-based alloy. It has cobalt; chromium is the maximum element. Stellite is a material, which is widely popular in the welding or cladding process because of its excellent corrosion control, wear &erosion properties. AISI/SS316L is a low-carbon austenite stainless steel. Fe and Cr elements are the major. In this work, stellite-6 filler wire of $\phi 1.2$ mm diameter is a cladding material over AISI316L substrate of size 200 mm x 420 mm. Table 1 shows the chemical compositions of the metals used for this study. The cladding was taken place by using a CMT welding machine based on the central composite design (CCD). Torch angle (deg.), welding speed (m/min), current (Amps.), and volts (V) were the welding parameters, and their values are given in table 2. Total 31 nos. of cladding experiments were done. The specimens for the testing and the characterization were cut by an EDM machine and polished using sandpaper and a polishing machine. The aqua regia etchant was used. The specimens of the experiments with first rank, middle rank, and last rank were characterized for analyzing their weld bead, corrosion analysis, and their microstructures. The optical microscope of Model: Dewinter optical tech and scanning electron microscope attached with EDS set up Model: Geminis SEM 300, Carlzeiss were used. The elemental distributions were confirmed through EDS spectra at the weld interface and base metal regions. Vickers microhardness was studied along with the base metals and the clad interface with a load of 1 kg and 10 seconds dwell time by Vickers hardness tester (INNOVATEST). Electrochemical impedance-CHI660A was used for the Corrosion study. COPRAS MCDM methodology was used for the optimization.

III. RESULTS AND DISCUSSION
A. COPRAS optimization
The selection of the best combinations of welding parameters is important when there are several alternative parameters combinations are present. Determining the best

combination of parameters from all available options is the MCDM problem [17, 18]. Generally, a problem in MCDM is articulated comfortably in the matrix form as in equations 1 and 2.

$$D = \begin{array}{c} \\ P_1 \\ P_2 \\ . \\ . \\ P_m \end{array} \begin{array}{cccc} C_1 & C_2 & \dots & C_n \\ \begin{bmatrix} x_1(1) & x_1(2) & . & . & x_1(n) \\ x_2(1) & x_2(2) & . & . & x_2(n) \\ . & . & . & . & . \\ . & . & . & . & . \\ x_n(1) & x_n(2) & . & . & x_n(n) \end{bmatrix} \end{array} \quad (1)$$

$$W = [w_1 \, w_2 \, \dots \, w_m] \quad (2)$$

where P_1 , P_2 ,…, P_m are the possible parameter combinations (trial runs) among which the best parameter combination should be selected; C_1 , C_2 ,…, C_n are the criteria with these the performance alternatives can be determined; $x_i(j)$ is the rating/grading of the combination P_i With regard to C_j, and w_j is the weight of criterion C_j[19]. The systematic methodology used for selecting the more appropriate alternative using the COPRASmethod is described below. The step followed in this paper is as follows[20].

Step 1: First, the dependent parameters and independent parameters should be identified since those are essential to define the type of problem. The dependent parameters which need maximization function are regarded as the preferable parameters, and those required minimization functions are regarded as the least preferable/favorable parameters.

In the current study, the output parameters, namely depth of penetration and hardness, need to be maximized hence considered most preferable, and the remaining output parameters require minimization; hence they are considered as least preferable attributes. Optimizing the responses can increase the quality and productivity of the resulting product.

Step 2: The information related to the output responses is to be expressed in terms of a matrix which is often termed as decision matrix and has i rows (m - alternatives) and j columns (n - criteria).

$$[D_{31 \times 5}] = \begin{pmatrix} 2.744 & 31.618 & 351 & 0.000781 & 0.079 \\ . & . & . & . & . \\ . & . & . & . & . \\ . & . & . & . & . \\ 1.858 & 30.346 & 336 & 0.004062 & 0.054 \end{pmatrix} \quad (3)$$

The decision matrix $[D_{31 \times 5}]$ of the present work is given in Eq. (1).

Step 3: The decision matrix from the previous step is normalized, and its elements are calculated using the following formula [Eq. (2)][21]. The normalized matrix is denoted as N_{ij}.

$$N_{ij} = \frac{x_{ij}}{\sum_{i=1}^{m} x_{ij}} \quad j = 1, 2, \dots, n \quad (4)$$

The calculation of normalized data for the first and last elements is as follows

$$N_{1\times1} = \frac{2.744}{(2.744 + 1.625 + \cdots + 1.858)} = 0.0390$$

$$\vdots \qquad\qquad (5)$$

$$N_{31\times5} = \frac{0.054}{(0.079 + 0.05 + \cdots + 0.054)} \; j = 0.0264$$

$$[N_{31\times5}]$$
$$= \begin{pmatrix} 0.0390 & 0.0327 & 0.1818 & 0.0011 & 0.0311 \\ \cdot & \cdot & \cdot & \cdot & \cdot \\ \cdot & \cdot & \cdot & \cdot & \cdot \\ \cdot & \cdot & \cdot & \cdot & \cdot \\ 0.0264 & 0.0356 & 0.0313 & 0.0056 & 0.0212 \end{pmatrix} \quad (6)$$

The normalized decision matrix $[N_{31\times5}]$ is computed as shown in Eq. (6).

Step 4: Then, a weighted normalized decision matrix is derived with the multiplication of the elements of the normalized decision matrix by its respective weights.

$$W_{ij} = N_{ij} \times W_j \qquad (7)$$

Where the normalized matrix is N_{ij} and, the weight criteria are W_j. With the help of experts, the weights (W_j) of each criterion are decided. Since the depth of penetration and hardness are most preferable, they are given a weight of 0.35, and the remaining parameters are given a weight of 0.1. The elements of resulted matrix called weighted normalized matrix $W_{31\times5}$ are computed using Eq. (8).

$$W_{1\times1} = 0.0390 \times 0.35$$
$$W_{1\times2} = 0.0231 \times 0.1$$
$$W_{1\times3} = 0.0313 \times 0.35$$
$$W_{1\times4} = 0.0411 \times 0.1$$
$$\vdots \qquad\qquad (8)$$
$$W_{31\times5} = 0.0264 \times 0.1$$

$$[D_{31\times5}] = \begin{pmatrix} 0.0137 & 0.0037 & 0.0114 & 0.0001 & 0.0031 \\ \cdot & \cdot & \cdot & \cdot & \cdot \\ \cdot & \cdot & \cdot & \cdot & \cdot \\ \cdot & \cdot & \cdot & \cdot & \cdot \\ 0.0093 & 0.0036 & 0.0110 & 0.0006 & 0.0021 \end{pmatrix}$$

The final weighted normalized matrix $[W_{31\times5}]$ is shown in Eq. (9).

Step 5: The summation of weighted normalized responses over the beneficial criteria those need to be maximized are calculated for each experimental run. It is expressed as P_i and is calculated using the following equation [20].

$$P_i = \sum_{j=1}^{k} x_{ij} \qquad (10)$$

Were k = number (No.) of responses that need maximization. According to the present work, depth of penetration and hardness has to be maximized; therefore, all the P_i values are calculated using Eq(11).

$$P_1 = 0.0137 + 0.0114 = 0.0251$$
$$P_2 = 0.0081 + 0.0114 = 0.0195$$
$$\vdots \qquad\qquad (11)$$

$$P_{31} = 0.0093 + 0.0110 = 0.0202$$

Step 6: Similarly, R_i, which is the summation of weighted normalized responses over the non-beneficial criteria those need to be minimized, are calculated using the Eq (12) as follows[22],

$$R_i = \sum_{j=n+1}^{m} x_{ij} \qquad (12)$$

In the above equation, (m – k) is the number of responses that require minimization. In the current study, the responses other than depth of penetration and hardness have to be minimized due to their unfavorable features.

$$R_1 = 0.0037 + 0.0001 + 0.0031 = 0.0069$$
$$R_2 = 0.0023 + 0.0006 + 0.0020 = 0.0049$$
$$\vdots \qquad\qquad (13)$$
$$R_{31} = 0.0036 + 0.0006 + 0.0021 = 0.0062$$

Step 7: Identification of the minimum value of R_i.

$$R_{min} = \min_i R_i, where\ i = 1, 2, \dots, m \qquad (14)$$

$$R_{min}$$
$$= \min(0.0069, 0.0049, \dots, 0.0062) \qquad (15)$$
$$= 0.0045$$

Step 8: Providing relative weight for each responses Q_i. The important relative value of response illustrates the measure of satisfaction achieved by that response. The larger the value of Q_i denotes the highest priority of the alternative, i.e., the experimental run. Hence the ranking of other parameter choices is done on the basis of a maximum of the largest relative value Q_{max}[22].

$$Q_i = P_i + \frac{R_{min} \sum_{i=1}^{m} R_i}{R_i \sum_{i=1}^{m} \frac{R_{min}}{R_i}} \qquad (16)$$

$$\sum_{i=1}^{m} R_i = (0.0069 + 0.0049 + \cdots$$
$$+ 0.0062) = 0.3000 \qquad (17)$$

$$\sum_{i=1}^{m} \frac{R_{min}}{R_i} = \left(\frac{0.0045}{0.0069} + \frac{0.0045}{0.0049} + \cdots \right.$$
$$\left. + \frac{0.0045}{0.0062} \right) = 18.055 \qquad (18)$$

The relative weights can be calculated using Eq (16) by applying the values calculated from Eq. (17) and Eq. (18), as presented in Eq. (19).

$$Q_1 = 0.0251 + \frac{0.0045 \times 0.300}{0.0069 \times 18.055}$$
$$= 0.0359$$

$$Q_2 = 0.0195 + \frac{0.0045 \times 0.300}{0.0049 \times 18.055}$$
$$= 0.0347 \qquad (19)$$

$$\vdots$$

$$Q_{31} = 0.0202 + \frac{0.0045 \times 0.300}{0.0062 \times 18.055}$$
$$= 0.0321$$

On the other hand, some researchers adopt the Eq.(20) for computing relative weights. However, both the equations result in the same values.

$$Q_i = P_i + \frac{\sum_{i=1}^{m} R_i}{R_i \sum_{i=1}^{m} \frac{1}{R_i}} \qquad (20)$$

Step 9: Calculation of the optimality criterion Q_{max}

$$Q_{max} = \max_i Q_i , where \ i = 1, 2, ..., m \qquad (21)$$

$$Q_{max} = \max(0.0359, 0.0347, ... , 0.0321) \\ = 0.0386 \qquad (22)$$

Step 10: Ranking the alternative experimental runs, i.e., the various combination of process parameters. A total of 31 experimental runs are ranked based on the major weight (relative weight of response) Q_i, and the larger is the primary (rank) of the study.

Step11: Assessment of the degree of utility for each response to complete the ranking. It is done by effectively assessing the preferences of all responses are computed as follows [22]:

$$N_i = \frac{Q_i}{Q_{max}} \times 100\% \qquad (23)$$

Using Eq. (23), the degree of utility is calculated. These utility degree values of each experimental run (alternative) are range from 0% to 100%. Table 3 gives the ranking order of the COPRAS optimization.

$$N_1 = \frac{0.0359}{0.0386} \times 100 = 93 \ \%$$
$$N_2 = \frac{0.0347}{0.0386} \times 100 = 90 \ \% \qquad (24)$$
.
$$N_{31} = \frac{0.0321}{0.0386} \times 100 = 83 \ \%$$

From the confirmationstudies, reasonable combinations of input parameters can be sought to improve the quality of weld.According to the computed results, a complete prioritization of the alternatives (experimental runs) is obtained as 4, 10, 25, 7, 17, 15, 22, 3, 11, 5, 23, 30, 9, 31, 12, 21, 27, 1, 26, 8, 20, 18, 2, 14, 13, 28, 6, 16, 29, 24, and 19. The optimal experimental run is sequenced as follows 23>18> 8 > 1 > 27 >20> 13 >10>4>9> 2 >15>25> 24>6> 28>22>31 >5>16>7> 30 >21> 11>3>19>17> 26> 14> 29 > 12. It is clear that the best-combination of input parameters is identified in run 23, and the worst is in run 12.

The experimental run 23 is the best alternative with 100% utility degree(UD), whereas the 12th run is the worst combination with 55% UD. According to the best solution, the optimal combination of input parameters was identified with an input current of 160 Amp, voltage of 19 V, torch angle of 50 deg, and welding speed of 150 m/min. Therefore, it is emphasized to choose the above parameters to perform welding to improve the quality of the element. Again, characterization studies were carried out for three ranks of parameters such as first rank, middle rank, and last rank. The detailed discussion is presented below.

B. Vickers microhardness

Microhardness was analyzed on the specimens, and figure 1 shows the microhardness measurement on the specimens of experiment nos. 23 (first rank), 6 (middle rank) and 12 (last rank). Vickers hardness measurement at every micron level interval nearby the weld is helpful to easily understand the property of phases [23] and the hardening effect of the CMT process. The hardness was measured on the cladding side, interface, and SS316L base metals. The best alternative recorded for experiment 23 had a current of 160 Amps and voltage of 19 V with a minimum of 100 m/min welding speed. The low speed with the high current was recommended for the best properties. Experiment 6 was also having a high current of 180 Amps and a low speed of 125 m/min. The voltage and high current combination provided good results. Whereas the last rank of experiment 12 with high values of welding parameters like 180 Amp current, 21 V, and 175 m/min welding speed. From the results, it was observed that the high values of current, voltage, and speed were giving poor weld properties but gave maximum microhardness of around 360 Hv1.0 on the cladding side. But the first rank experiment yielded maximum microhardness in cladding, interface, and SS316L base sides.

C. Macrographs and Microstructure Characterization

The morphology study was done on the specimens. The researchers are recommending the macro and micro study of AISI316L alloy after the heat applied processes like welding [24]. The macrographs of experiment no. 6 (middle rank), 12 (last rank), and 23rd (first rank) are shown in figure 2 (a-c). From the macrographs, no defects were found. The bead width and the bead height are almost the same for all the experiments. While looking at the molten zone in base metal, experiment 6 was having high than the other experiments 12, 23. The molten zone is available below the fusion line. The 6th experiment had a higher current of 180 Amps. A higher current can lead to having a higher molten zone. The weld bead is also bigger than the others. The weld bead is to be considered for analyzing the property of the cladding. The cross-section area of the bead is small for experiment 23. The heat-damaged/affected zone (HAZ) and fusion zone/region are also seen in the macrographs. Higher current and welding speed and the higher voltage produced large weld beads. However, the low welding speed produced a small weld bead with a low fusion zone. From the results, a low welding current with 160 Amp current is recommended. The austenitic structure was observed in the base material SS316L alloy. This structure was known on the specimen before the cladding by CMT took place. The structures of the cladding portions obtained through an optical microscope (OM) are shown in figures 2 (d-f) for the specimens' experiments 6, 12, and 23, respectively.

Figures 3a-f show the scanning electron microstructure (SEM) images of the weld interfaces and cladding surface of the specimens. Figure 3a, b is for

experiment 6, which is the 15th rank (middle rank). Figure 3c, d is for experiment 12, which is the 31st rank (last rank). Figure 3e, f is for the 23rd experiment, which is the 1st rank according to COPRAS optimization. The microstructure consists of the hard phases like Cr and Co phase structure. The boundary was good and had good bonding between SS316L and stellite-6. In figure 3b, the fusion zone is shown. The size and the shape of the fusion region varied according to the welding parameters. Cr phase structure was uniform, as shown in figure 3b. The very narrow interfaces have been seen in figures 3a, 3c, and 3e. The grain boundary of the structure is also seen in figure 3d. The length of the grain is around 10 microns. The Cr-Co phase thickness is very narrow and around 1-2 microns. The dendrite structure is found in the cladding portion. This hard structure can alter the property and improve the wear resistance. The SEM images showed no defects in the interface and cladding portion. The interface thickness was measured, and the values are in the range of 0.04 mm -0.19mm. The Cr-based structure is almost uniform in all experiments. The structure and the size and thickness of Cr, Co-based phases in the filament form are slightly varying according to the weld parameters variables. The dendrite structure is found in the cladding portion. The hard surface is well established due to their Co phases and the corrosion resistance owing to the availability of the Cr phase. Experiment 23 attained 1st rank when optimizing the parameter using the COPRAS method.

Figure 4 is the SEM structure of the cladding surface, and figures 4 b & c show their EDS spectra. The EDS was analyzed in the coated surface, and the spectra were taken in regions A and B, as shown in the SEM image. It showed the elements present. From figure 4b, at EDS 'A' region consists of a maximum of cobalt up to 39%, followed by Fe and Cr. Whereas from figure 4c, at EDS, 'B' has a major of chromium 37%, followed by Co. The less amount of manganese only found in the regions. While comparing both EDS regions A and B, region B has less iron (Fe) content.

D. Corrosion rate analysis

It is needed to analyze the corrosion property of the cladding part as its application is valuable in industries [25]. The corrosion property was analyzed on the specimens of experiments 6, 12, and 23. Experiment 6 (Middle rank) showed the value of 0.009029 mm/yr corrosion rate, the corrosion rate of the specimen for experiment 12 (last rank) was 0.08392 mm/yr, and the experiment 23rd with first-rank showed a very less corrosion rate of 0.000853 mm/yr. The low welding speed improved corrosion resistance. The high voltage, high welding speed, and high welding current, as in experiment 12, increased the corrosion rate of the specimens shown in figure 5a. The corroded specimens were analyzed under SEM equipment, and while analyzing the corroded parts, the corrosion rate was high for experiment 12, as shown in figure 5b. The cladding portion showed good corrosion resistance as it had Cr and Co-based structure on its surface.

IV. CONCLUSIONS

In this work, the stellite-6 cladding was successfully made over the alloy AISI316L alloy by the process CMT, and the COPRAS methodology was used for the optimization of welding parameters. Through the optimization, the first, middle, and last ranks were sorted out from the list of experiments, and then their specimen was characterized. This work is helpful in industries to design a welding process with new materials to obtain maximum efficiency and to reduce distortion. The following conclusions were made from this investigation.

a) COPRAS methodology can be applied in welding engineering to find the best alternatives.

b) CMT process is suitable for the welding combination of stellite-6 and AISI316L alloys.

c) Experiment 6 is the 15th rank, i.e., middle rank, exp. No. 12 is the last rank, and the properties of exp. No. 23 attained the first rank as per COPRAS optimization.

d) Depth of penetration, weld area, and / interface thickness was measured, and the data are presented in this paper. The experiment 23rd has the minimum weld interface thickness of 0.048 mm

e) Experiment 23 attained the first rank with 160 Amps welding current and a low welding speed of 100 m/min.

f) The experiment with the first rank yielded a maximum microhardness at cladding, interface, and stainless steel base metals. The hardness was varied at the sides depending on the changes in their welding parameters values. The cladding part showed 350 Hv for experiments 12 & 23.

g) The corrosion rate is very less at 0.000853 mm/yr for the 23rd experiment.

h) The weld bead morphology depended on the welding parameters, and the molten zone in the base alloy is small for experiment 23 compared to experiments 6 and 12.

i) The higher current and the higher welding speed yielded a large weld bead and a higher fusion zone.

j) From the macrographs, no defects were found in the cladding, interface, and SS316L sides. EDS showed the presence of Cr, Co elements in the cladding surface.

REFERENCES

[1] Zavadskas, E. K., Kaklauskas, A. & Sarka, V. The new method of multicriteria complex proportional assessment of projects. Technological and economic development of the economy, 1(1994) 131-139.

[2] Alinezhad A., Khalili J. COPRAS Method. In: New Methods and Applications in Multiple Attribute Decision Making (MADM). International Series in Operations Research & Management Science. Iran: Springer'(2019).

[3] Zavadskas, E. K., Kaklauskas, A., Turskis, Z. & Tamošaitienė, J. Multi-attribute decision-making model by applying for grey numbers. Informatica, 20(2) (2009) 305-320.

[4] Saad, M. H., Nazzal, M. A. & Darras, B. M. A general framework for sustainability assessment of manufacturing processes. Ecological Indicators. 97 (2019) 211-224.

[5] Audrius Čereška, AskoldasPodviezko, Edmundas Kazimieras Zavadskas, Assessment of Different Metal Screw Joint Parameters by Using Multiple Criteria Analysis Methods, Metals. 8(5) (2018) 318.

[6] Jagannath Roy, Haresh Kumar Sharma, Samarjit Kar, Edmundas Kazimieras Zavadskas & Jonas Saparauskas An extended COPRAS model for multi-criteria decision-making problems and its application in web-based hotel evaluation and

selection, Economic Research-Ekonomska Istraživanja.; 32(1) (2019) 219-253.

[7] S.Nweze and J. Achebo, Comparative enhancement of mild steel weld mechanical properties for better performance using COPRAS-ARAS method. European journal of engineering and technology research. 6(2) (2021).

[8] M. Gomathisankar, M. Gangatharan, P. Pitchipoo, A Novel Optimization of Friction Stir Welding Process Parameters on Aluminum Alloy 6061-T6, Materials Today: Proceedings. 5(6) (2018) 14397-14404.

[9] Makhesana, M.A., Application of improved complex proportional assessment (COPRAS) method for rapid prototyping system selection, Rapid Prototyping Journal, 21 (6) (2018) 671-674.

[10] Subramanian, S.M., Paulraj, S. & Abdul Haq, N.H. Effect of faying surfaces and characterization of aluminum AA6063–steel AISI304L dissimilar joints fabricated by friction welding with hemispherical bowl and threaded faying surfaces. Int J Adv Manuf Technol (2021).

[11] P.Ganesh, A. Moitra, Pragya Tiwari, S. Sathyanarayanan, Harish Kumar, S.K. Rai, Rakesh Kaul, C.P. Paul, R.C. Prasad, L.M. Kukreja Fracture behavior of laser-clad joint of Stellite 21 on AISI 316L stainless steel, Materials Science and Engineering: A, 527(16–17) (2010) 3748-3756.

[12] A. Shahroozi, A. Afsari, B. Khakan, A.R. Khalifeh, Microstructure, and mechanical properties investigation of stellite 6 and Stellite 6/TiC coating on ASTM A105 steel produced by TIG welding process, Surface and Coatings Technology, 350 (2018) 648-658.

[13] Rajeev G.P., Kamaraj M., Srinivasa R. Bakshi, Hardfacing of AISI H13 tool steel with Stellite 21 alloy using cold metal transfer welding process, Surface and Coatings Technology, 326(A) (2017) 63-71.

[14] F. Madadi, F. Ashrafizadeh, M. Shamanian, Optimization of pulsed TIG cladding process of stellite alloy n carbon steel using RSM, Journal of Alloys and Compounds, 510(1) (2012) 71-77.

[15] Dariusz Bartkowski, Andrzej Młynarczak, Adam Piasecki, Bartłomiej Dudziak, Marek Gościański, Aneta Bartkowska, Microstructure, microhardness and corrosion resistance of Stellite-6 coatings reinforced with WC particles using laser cladding, Optics & Laser Technology, 68 (2015) 191-201.

[16] Anish Nair, V. Ramji, R. Durai Raj, R. Veeramani, Laser cladding of Stellite 6 on EN8 steel – A fuzzy modeling approach, Materials Today: Proceedings, 39(1) (2021) 348-353.

[17] Vipul Gupta, Babalukumar, Uttam Kumar Manda, CNC Machine tool selection using MCDM techniques and application of software SANNA, International Journal of Engineering Trends and Technology (IJETT) – 35(7) (2016) 323-334.

[18] Omar Mohd Faizan Bin Marwah, AdilahBintiDarsani, Mohd Yussni Bin Hashim, Elmy Johana Binti Mohamad, A Response Surface Methodology Approach for The Optimisation of Energy and Waste Manufactured by Portable3D Printing International Journal of Engineering Trends and Technology 68(12) (2020) 113-117.

[19] Peng, C., Du, H. & Warren Liao, T. A research on the cutting database system based on machining features and TOPSIS. Robotics and Computer-Integrated Manufacturing, 43 (2015) 96-104.

[20] Yazdani, M., Alidoosti, A. & Zavadskas, E. K. Risk analysis of critical infrastructures using fuzzy COPRAS. Economic research-Ekonomska istraživanja, 24(4) (2011) 27-40.

[21] Singaravel, B. & Selvaraj, T. Optimization of machining parameters in turning operation using combined TOPSIS and AHP method. Tehnicki Vjesnik. 22 (2015) 1475-1480.

[22] Adali, E. A. & Işik, A. T. Air conditioner selection problem with COPRAS and ARAS methods. Manas Sosyal Araştırmalar Dergisi, 5(2) (2016) 124-138.

[23] Senthil Murugan S, Sathiya P, Noorul Haq A, Experimental Study on the Effect of Silver, Nickel, and Chromium Interlayers and Upset Pressure in Joining SS304L-AA6063 Alloys through Direct Drive Friction Welding Process. Journal of the Brazilian Society of Mechanical Sciences and Engineering, 42(611) (2020) 1-17.

[24] Wichan Chuaiphan, Loeshpahn Srijaroenpramong, Evaluation of microstructure, mechanical properties and pitting corrosion in dissimilar of alternative low-cost stainless steel grade 204Cu and 304 by GTA welding joint, Journal of Materials Research & Technology, 9(3) (2020) 5174-5183.

[25] Zhaohui Tian, Lijun Song, Xinmin Li, Effect of Oxidizing Decontamination Process on Corrosion Property of 304L Stainless Steel, International Journal of Corrosion, 2019(1206098) (2019) 6.

Table 1: Chemical composition of metals (Elements in Wt. %)

Filler Wire: Stellite 6

Cr	*W*	*C*	*Fe*	*Si*	*Mn*	*Co*			
28	4	1.15	1.3	1.1	0.06	Bal.			

Base Material: AISI/SS 316L

C	*Mn*	*Si*	*Cr*	*Ni*	*Mo*	*P*	*S*	*N*	*Fe*
0.03	2	0.75	16-18	10-14	2-3	0.045	0.03	0.1	Bal.

Table 2: Welding Parameter and the Level

Parameters	Notations	-2	-1	0	+1	+2
Torch Angle (deg)	TA	50	60	70	80	90
Welding Current (Amps)	I	120	140	160	180	200
Welding Speed (m/min)	TS	100	125	150	175	200
Voltage (v)	V	15	17	19	21	23

Table 3: Relative weight, utility degree, and its rank

| Number of runs	R_i	R_{min}/R_i	Q_i	N_i	Rank	Number of runs	R_i	R_{min}/R_i	Q_i	N_i	Rank
1	0.0070	0.6505	0.0363	93%	4	17	0.0207	0.2195	0.0270	69%	27
2	0.0052	0.8673	0.0343	88%	11	18	0.0051	0.8840	0.0390	100%	2
3	0.0115	0.3944	0.0293	75%	25	19	0.0246	0.1847	0.0274	70%	26
4	0.0086	0.5263	0.0350	90%	9	20	0.0062	0.7369	0.0356	91%	6
5	0.0089	0.5125	0.0318	81%	19	21	0.0113	0.4010	0.0304	78%	23
6	0.0099	0.4597	0.0328	84%	**15**	22	0.0066	0.6920	0.0326	83%	17
7	0.0079	0.5731	0.0308	79%	21	23	0.0045	1.0000	0.0390	100%	**1**
8	0.0066	0.6834	0.0367	94%	3	24	0.0067	0.6795	0.0329	84%	14
9	0.0068	0.6645	0.0347	89%	10	25	0.0071	0.6423	0.0337	86%	13
10	0.0088	0.5151	0.0353	90%	8	26	0.0113	0.4003	0.0269	69%	28
11	0.0124	0.3671	0.0303	78%	24	27	0.0051	0.8853	0.0358	92%	5
12	0.0222	0.2042	0.0251	64%	**31**	28	0.0067	0.6783	0.0327	84%	16
13	0.0057	0.7943	0.0355	91%	7	29	0.0153	0.2974	0.0254	65%	30
14	0.0127	0.3566	0.0258	66%	29	30	0.0083	0.5467	0.0305	78%	22
15	0.0077	0.5911	0.0343	88%	12	31	0.0065	0.6941	0.0321	82%	18
16	0.0119	0.3819	0.0309	79%	20						
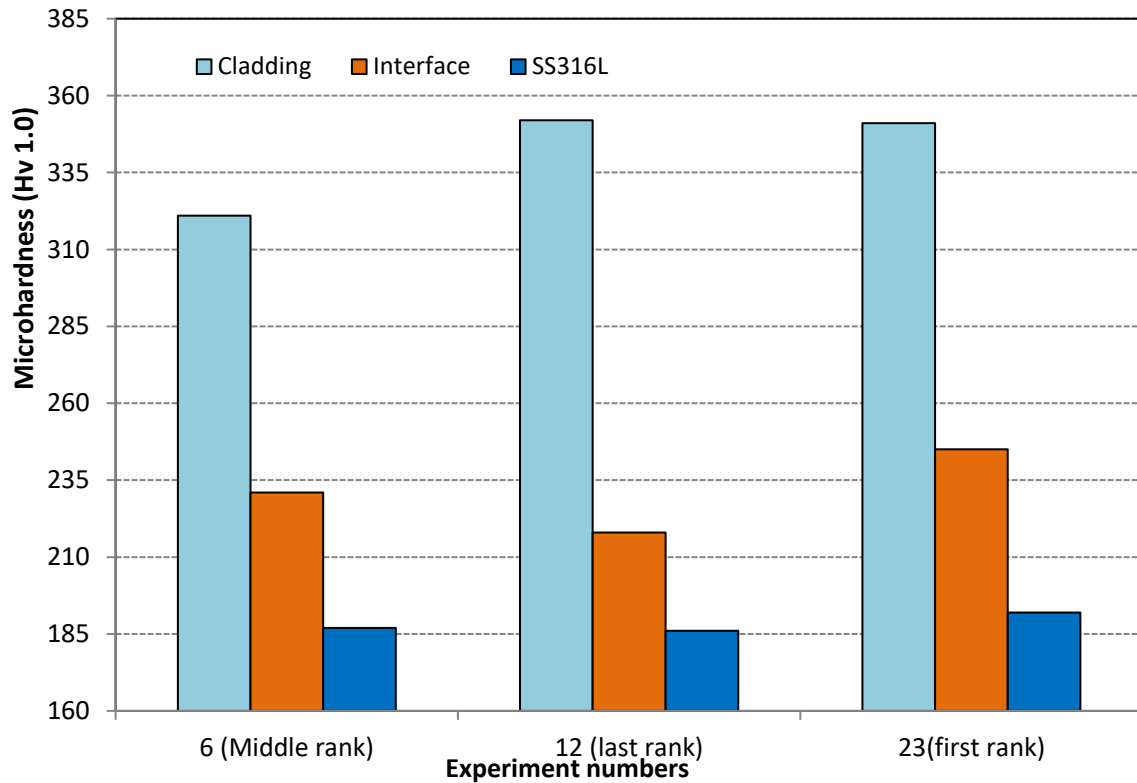
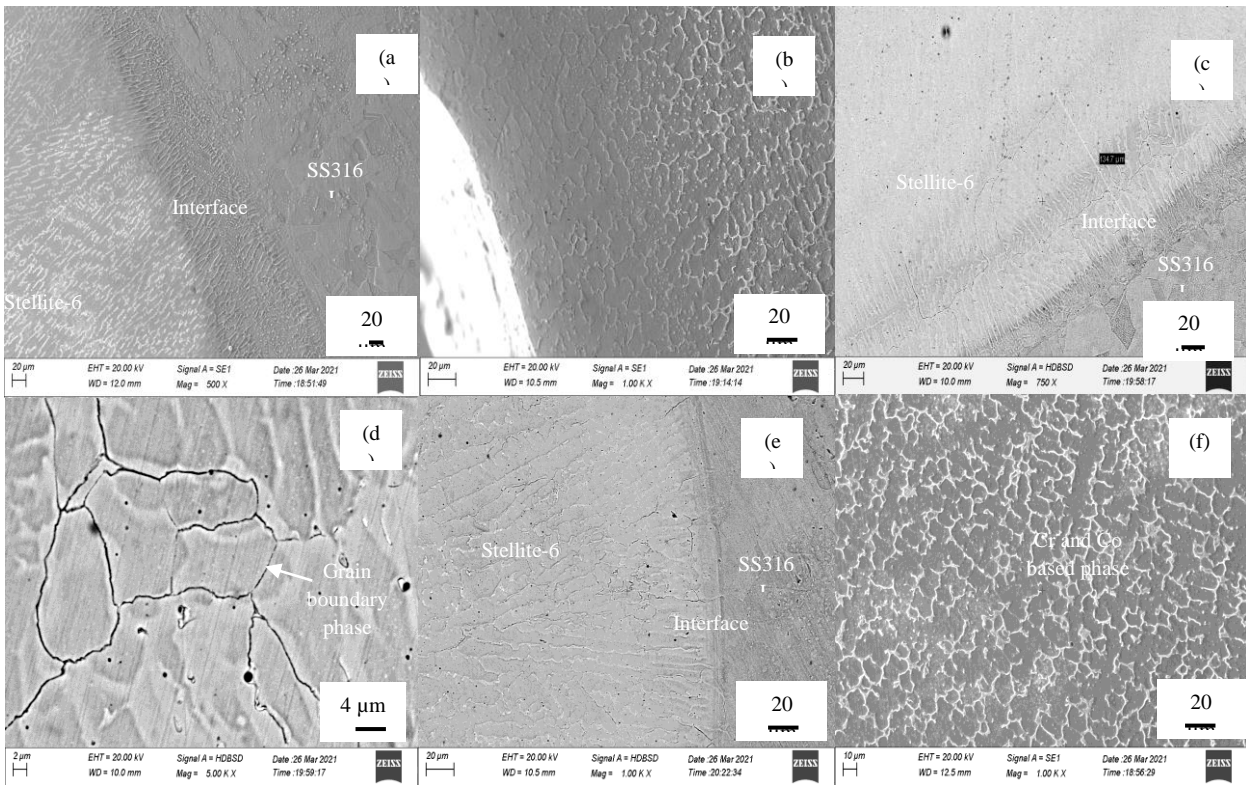**Figure 1: Microhardness Measurement along metal SS316L, interface & Cladding areas**
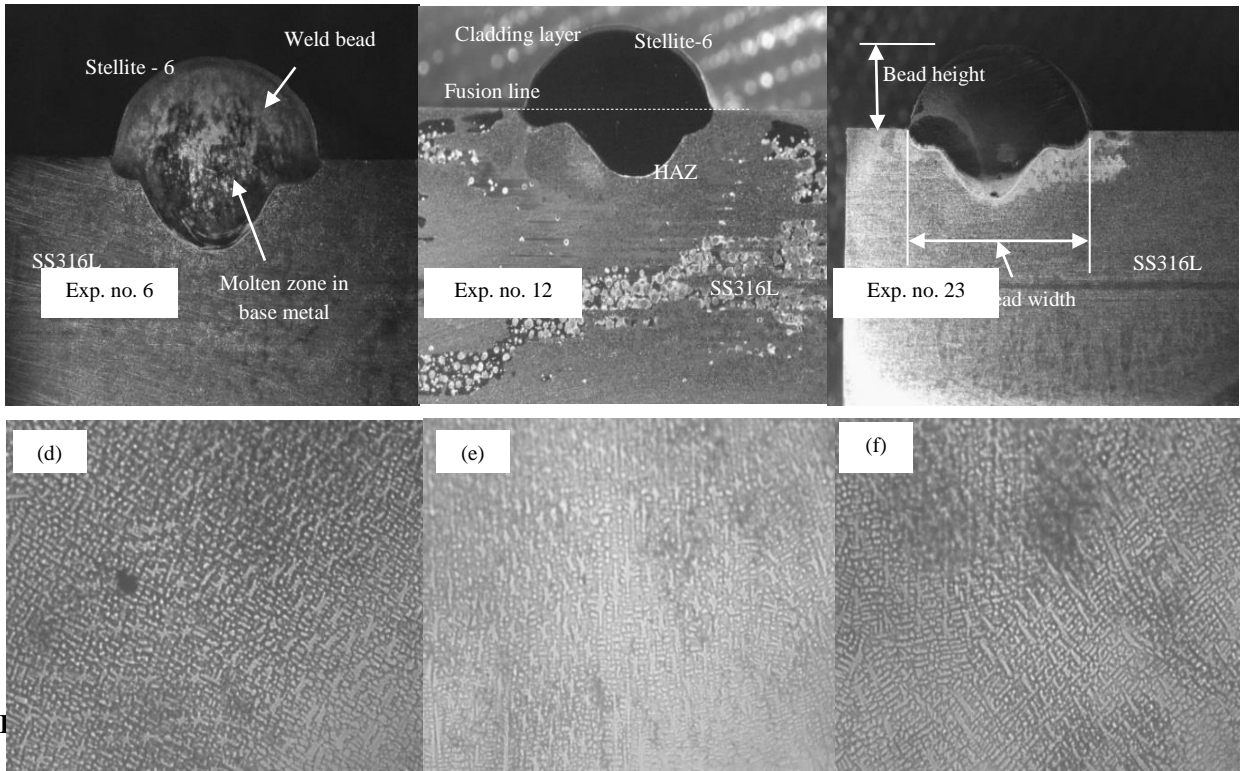
Figure 3(a-f): SEM images of interface and cladding portion, (a-b) Exp no 6, (c-d) Exp no 12, (e-f) Exp no 23
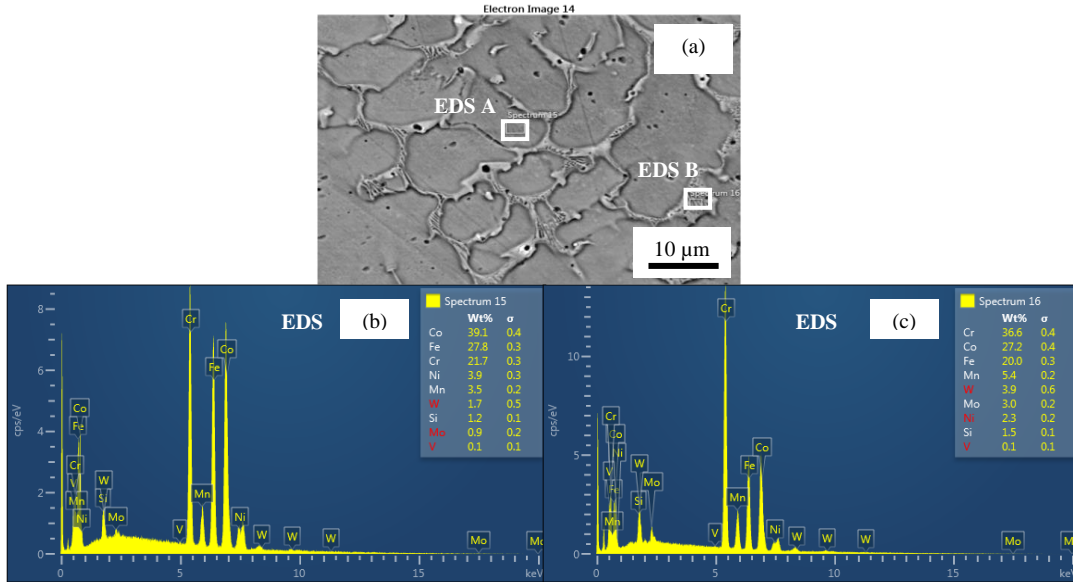
Figure 4(a-c): a) SEM of stellite-6 cladding of experiment 23, b, c) EDS spectra in Cr and Co phases
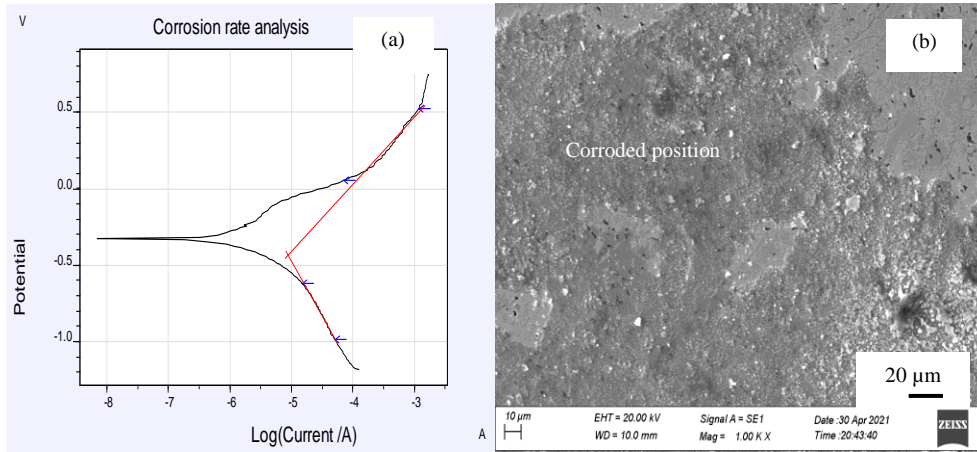
Figure 5: a) Corrosion rate analysis reports & b) SEM images of Corroded specimens of Sample 12